New Structural Scaffolds for Centrally Acting Oxime Reactivators of Phosphylated Cholinesterases[*][S]

Rakesh K. Sit[‡], **Zoran Radić**[§], **Valeria Gerardi**[§], **Limin Zhang**[§], **Edzna Garcia**[§], **Maja Katalinić**[¶], **Gabriel Amitai**[‖], **Zrinka Kovarik**[¶], **Valery V. Fokin**[‡], **K. Barry Sharpless**[‡], and **Palmer Taylor**[§1]

From the [‡]Department of Chemistry and the Skaggs Institute for Chemical Biology, The Scripps Research Institute, La Jolla, California 92037, the [§]Skaggs School of Pharmacy and Pharmaceutical Sciences, University of California at San Diego, La Jolla, California 92093, the [¶]Institute for Medical Research and Occupational Health, HR-10001 Zagreb, Croatia, and the [‖]Department of Pharmacology, Israel Institute for Biological Research, Ness Ziona 74100, Israel

We describe here the synthesis and activity of a new series of oxime reactivators of cholinesterases (ChEs) that contain tertiary amine or imidazole protonatable functional groups. Equilibration between the neutral and protonated species at physiological pH enables the reactivators to cross the blood-brain barrier and distribute in the CNS aqueous space as dictated by interstitial and cellular pH values. Our structure-activity analysis of 134 novel compounds considers primarily imidazole aldoximes and N-substituted 2-hydroxyiminoacetamides. Reactivation capacities of novel oximes are rank ordered by their relative reactivation rate constants at 0.67 mM compared with 2-pyridinealdoxime methiodide for reactivation of four organophosphate (sarin, cyclosarin, VX, and paraoxon) conjugates of human acetylcholinesterase (hAChE). Rank order of the rates differs for reactivation of human butyrylcholinesterase (hBChE) conjugates. The 10 best reactivating oximes, predominantly hydroxyimino acetamide derivatives (for hAChE) and imidazole-containing aldoximes (for hBChE) also exhibited reasonable activity in the reactivation of tabun conjugates. Reactivation kinetics of the lead hydroxyimino acetamide reactivator of hAChE, when analyzed in terms of apparent affinity ($1/K_{ox}$) and maximum reactivation rate (k_2), is superior to the reference uncharged reactivators monoisonitrosoacetone and 2,3-butanedione monoxime and shows potential for further refinement. The disparate pH dependences for reactivation of ChE and the general base-catalyzed oximolysis of acetylthiocholine reveal that distinct reactivator ionization states are involved in the reactivation of ChE conjugates and in conferring nucleophilic reactivity of the oxime group.

It has become increasingly apparent that efficient reinstatement of CNS acetylcholinesterase (AChE)[2] activity inhibited in organophosphate (OP)-intoxicated individuals is required for sustained symptom recovery. In particular, nerve agent OPs already used by terrorists, but also active metabolites of OP-based pesticides, readily cross the blood-brain barrier (BBB). The exposure to OP doses close to lethality results in initial severe motor convulsions and epileptic seizures. Accumulating evidence points to these seizure events being linked to irreversible long term compromise of cognitive functions and alteration of CNS electrical excitability. Once accumulated into hydrophobic sites, OPs that do enter the CNS are retained and partition slowly back into the circulation. For example, victims of Tokyo subway nerve gas attack in 1995 were found to suffer from both short and long term symptoms of OP exposure (1–4). Accordingly, comprehensive protection from and treatment of OP intoxication to minimize the longer term consequences require administration of antidotes capable of reactivating OP-inhibited AChE in the CNS.

Current therapy directed to reactivating inhibited AChE is limited to the peripheral circulation because commonly used quaternary pyridinium aldoxime reactivators do not cross the BBB at therapeutically relevant levels (5). Only a handful of studies involving centrally acting reactivators have been reported in the literature, including nonspecific acetyloxime derivatives 2,3-butanedione monoxime (DAM) and monoisonitrosoacetone (MINA) (6–8), glycosylated pyridinium oximes (9, 10), and dihydropyridine prodrug, pro-2PAM (2-pyridinealdoxime methiodide) derivatives (11, 12). Studies involving pro-2PAM have yielded most promising OP protection results, yet even with efficient or immediate conversion in the CNS, pro-2PAM is inherently limited by reactivation efficacy of 2PAM itself.

To improve reactivation therapy in the CNS, we initiated a program to develop, by significantly expanding existing reactivator chemical space, centrally active AChE reactivators devoid of permanent positive charge, but amenable to protonation (Scheme A). The uncharged species of reactivators are expected to diffuse across the BBB into the CNS, and upon establishing the pH-dependent equilibrium between the neutral and ionized forms in extracellular CNS space, the protonated form would efficiently interact with the electron-rich active center environ-
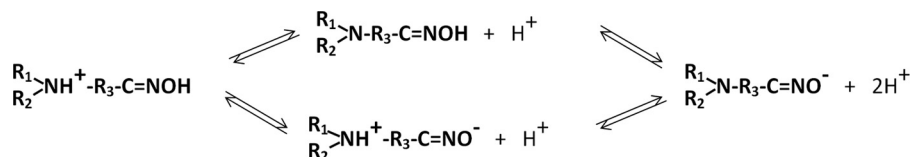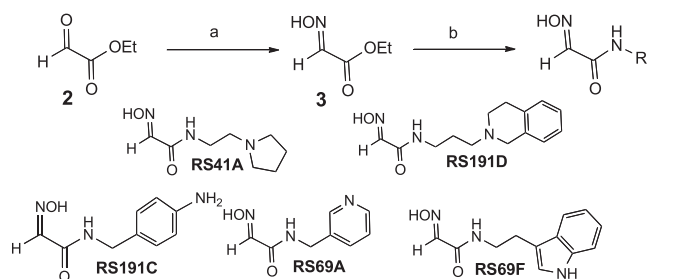
SCHEME A. Generalized ionization equilibria of amino oximes with two ionizing groups proceeds through formation of a neutral or zwitterionic species.
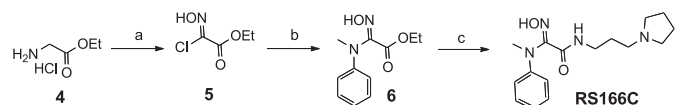

R^1=Hex(**RS113A**), Pent(**RS113B**),
Bu(**RS115A**), Pr(**RS115B**), Et(**RS115C**)
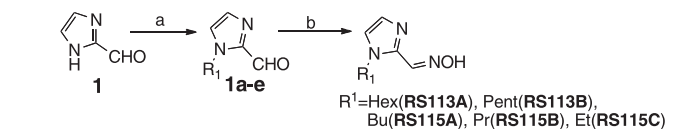
Reagents: (a) R^1Br, K_2CO_3, DMF, 50 °C; (b) $NH_2OH \cdot HCl$, H_2O, Na_2CO_3, 70 °C

SCHEME 1

Reagents: (a) $NH_2OH \cdot HCl$, Et_3N, CH_3CN, H_2O, rt; (b) RNH_2, C_2H_5OH, 50 °C

SCHEME 2

Reagents: (a) HCl, $NaNO_2$, H_2O, -5 °C (b) *N*-methylaniline, Et_3N, Et_2O, rt;
(c) 3-(pyrrolidinyl)propanamine, C_2H_5OH, 50 °C

SCHEME 3

Reagents: (a) Azidoalkyl methanesulfonate, K_2CO_3, DMF 50 °C; (b) $NH_2OH \cdot HCl$, H_2O,
Na_2CO_3, 70 °C; (c) $CuSO_4$, sodium ascorbate, t-BuOH/H_2O (2:1), 50 °C

SCHEME 4

Reagents: (a) Propargyl amine, C_2H_5OH, rt; (b) $CuSO_4$, sodium ascorbate, t-BuOH/H_2O
(2:1), 50 °C

SCHEME 5

Reagents: (a) Propargyl methanesulfonate, K_2CO_3, DMF, 50 °C; (b) $NH_2OH \cdot HCl$, H_2O, Na_2CO_3,
70 °C; (c) CuI, (*i*-Pr)$_2$NH, MeOH/THF, rt

SCHEME 6
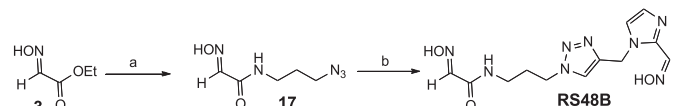
Reagents: (a) 3-azidopropyl-1-amine, C_2H_5OH, rt; (b) $CuSO_4$, sodium ascorbate, t-BuOH/H_2O
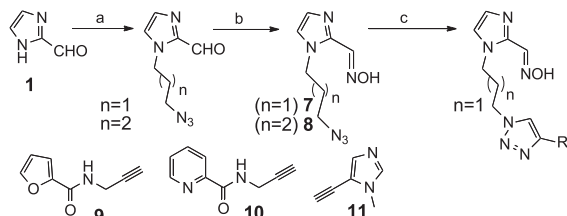(2:1), 50 °C

SCHEME 7

ment of the OP-inhibited AChE. Accordingly, reactivating amines or imines with pK_a values between 7 and 10 would exhibit optimal ionization equilibrium characteristics.

Here, we report design, synthesis, and initial functional characterization of 134 novel oxime reactivators that remain largely neutral at physiological pH values. Oxime-elicited reactivation rates were determined at a single concentration for paraoxon-, sarin-, VX-, and cyclosarin-inhibited recombinant human AChE (hAChE). For the 10 best reactivators, we examined reactivation of tabun-inhibited conjugates. In addition, the majority of oximes were screened for reactivation of paraoxon-, sarin-, VX-, and cyclosarin-inhibited human butyrylcholinesterase (hBChE) to assess the breadth of conjugates that show significant reactivation.

Our considerations of structure and pH dependence of reactivation provide evidence that oxime access to the phosphonyl or phosphoryl phosphorous atom within the narrow confines of the gorge appears to be the critical criterion for efficient reactivation, rather than the ionization state governing oximate formation.
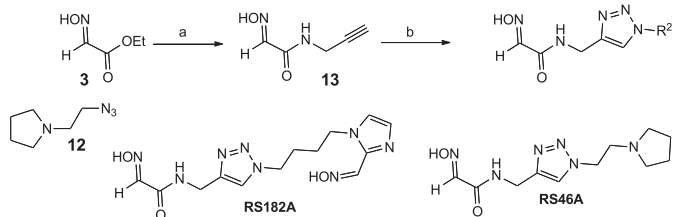
MATERIALS AND METHODS

Enzymes—Monomeric hAChE was expressed in stably transfected HEK-293 cells (American Type Culture Collection, Manassas, VA) obtained upon calcium phosph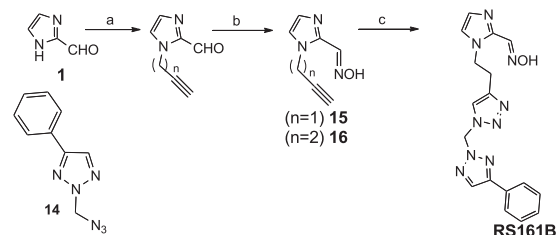ate transfection with pCMV-N-FLAG (Sigma-Aldrich) construct of hAChE encoding cDNA with a stop codon truncating the sequence at amino acid 547. Selection of neomycin-resistant cell colonies using G418 (Invitrogen) enhanced expression. The expressed
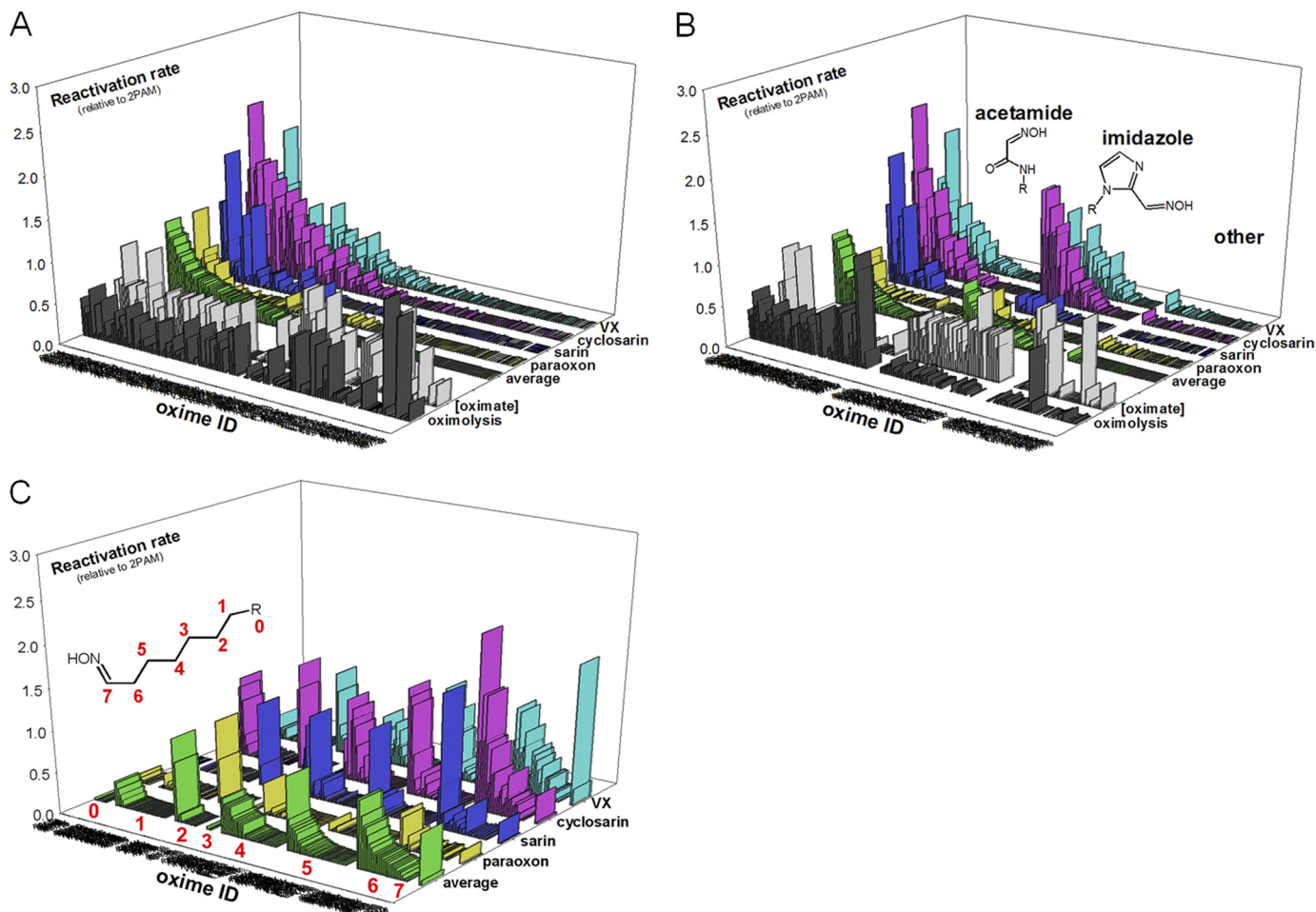
FIGURE 1. Reactivation of VX-, cyclosarin-, sarin-, and paraoxon-inhibited hACHE by library of 134 uncharged oxime reactivators. Reactivation rates (k_{obs}) of 0.67 mM oximes (measured at 37 °C in 0.10 M phosphate buffer, pH 7.4) are given relative to 2PAM. Average reactivation potencies of oximes for all four organophosphates are shown as *green bars*. Oxime IDs are ordered by their average reactivity (*A*), segregated by their general structure as acetamide, imidazole, and other oximes (*B*), and segregated by length of a linker connecting an oxime nucleophile and part of the molecule "R" responsible for binding interaction with hACHE (*C*). Measured rates of oximolysis (3 × DA/min) and calculated fractions of oximate anion for pH 7.4 are also given as *black* and *gray bars*, respectively. Structures and reactivation potencies of all 134 oximes are given in supplemental Table S1.

secreted protein containing the N-terminal FLAG tag was purified in several milligram quantities by an anti-FLAG affinity column (Sigma-Aldrich). Purified oligomeric hBChE isolated from human plasma was kindly donated by Drs. Douglas Cerasoli and David Lenz, United States Army Medical Research Institute of Chemical Defense, Edgewood, MD.

Organophosphates—Nonvolatile, low toxicity fluorescent methylphosphonates (Flu-MPs) (13) were used as analogues of nerve agents sarin, cyclosarin, and VX. The Flu-MPs differ from actual nerve agent OPs only by structure of their respective leaving groups. Inhibition of ChEs by Flu-MPs results in OP-ChE covalent conjugates identical to the ones formed upon inhibition with nerve agents. Paraoxon was purchased from Sigma-Aldrich and tabun from NC Laboratory (Spiez, Switzerland).

Oximes—2PAM, MINA (monoisonitrosoacetone), and DAM (2,3-butanedione monoxime) were purchased from Sigma-Aldrich. The synthesis of imidazole aldoxime derivatives **RS113A**, **RS113B**, **RS115A**, **RS115B**, and **RS115C** is outlined in Scheme 1. Alkylation of 2-formylimidazole **1** with the requisite bromide followed by treatment with hydroxylamine delivered the desired oxime. See also supplemental Methods.

N-Substituted 2-hydroxyiminoacetamides **RS41A**, **RS191D**, **RS191C**, **RS69A**, and **RS69F** were prepared from ethyl glyoxylate **2** in two steps (Scheme 2). Condensation with hydroxylamine provided ethyl glyoxylate oxime **3** followed by subsequent amidation with the corresponding primary amine.

For the preparation of **RS166C**, glycine ester hydrochloride **4** was converted into 2-chloro-2-(hydroxyimino)acetate **5** (Scheme 3) (14). Treatment of **5** with *N*-methylaniline and triethylamine at room temperature afforded 2-amino-2-(hydroxyimino)acetate **6** (15). Amidation of **6** with 3-(pyrrolidinyl)propanamine delivered acetamide oxime **RS166C**.
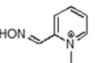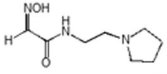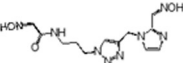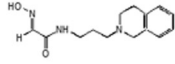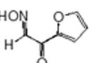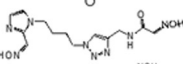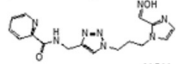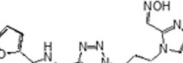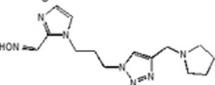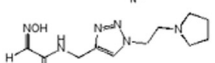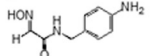
Azido intermediates **7** and **8** were synthesized from formylimidazole **1** by alkylation with azidoalkylmethanesulfonate followed by condensation with hydroxylamine (Scheme 4). Imidazole-1,4-triazole derivatives **RS185B**, **RS150D**, and **RS210B** were then subsequently obtained via a Cu-catalyzed azide alkyne cyclo addition (CuAAC) (16) between azido derivative **7** and corresponding alkyne derivatives **9** (17), **10** (18), and **11**, respectively.

The 1,4-triazole oxime derivatives **RS146A** and **RS182A** were prepared as illustrated in **Scheme 5**. Amidation of ethyl glyoxylate oxime **3** with commercially available propargyl

TABLE 1

Structures and relative rate constants for OP-hAChE reactivation (k_{obs}) of 10 topmost uncharged reactivators (0.67 mM) compared with cationic pyridinium aldoxime 2PAM

Nonenzymic oximolysis rates of ATCh (1 mM) by 1.0 mM oximes and calculated percentages of oximate anion and neutral species at pH 7.4 (calculated by MarvinView 5.2.6) are also given. Experiments were performed in duplicate at 37 °C in 0.10 M phosphate buffer, pH 7.4.

Oxime	Oxime structure	k_{obs} (relative to 2PAM)*						Oximo lysis (dA/min)	% Oximate @ pH 7.4	% Neutral @ pH 7.4
		Avrg	POX	Sarin	CS	VX	Tabun			
2PAM		1.00	1.0	1.0	1.0	1.0	1.00	0.157	17	0.0
RS41A		0.72	0.10	1.0	1.3	1.1	0.08	0.120	0.20	7.0
RS48B		0.67	0.034	0.50	2.1	0.64	0.06	0.098	56	0.0
RS191D		0.66	0.14	1.61	0.48	1.0	0.07	0.103	0.29	6.5
RS186B		0.58	0.54	0.25	1.3	0.78	0.03	0.201	59	41
RS182A		0.55	0.14	0.25	0.34	1.7	0.33	0.140	100	0
RS150D		0.54	0.050	0.20	0.85	1.0	0.58	0.023	52	48
RS185B		0.53	0.38	0.19	1.4	0.54	0.16	0.022	52	48
RS185d		0.51	0.056	0.079	1.4	0.51	n.m.**	0.0240	53	24
RS46A		0.35	0.024	0.88	0.21	0.58	0.06	0.079	0.70	1.0
RS191C		0.34	0.38	0.60	0.50	0.24	0.00	0.167	0.20	99.8

* k_{obs} values determined for 2PAM were: 0.087 min^{-1} (for POX), 0.16 min^{-1} (for sarin), 0.025 min^{-1} (for CS), 0.15 min^{-1} (for VX) and 0.0026 min^{-1} (as 1.0 mM for tabun).
** Not measured.

amine provided intermediate **13**. The CuAAC reaction of **13** with **8** and **12** delivered triazole oxime derivatives **RS182A** and **RS46A**, respectively.

Azido derivative 2-(azidomethyl)-4-phenyl-2*H*-1,2,3-triazole **14** was prepared by treating phenyl acetylene with formaldehyde and sodium azide in a one-pot synthesis (19). The imidazole alkyne intermediates **15** and **16** were prepared in two steps (Scheme 6) by first alkylating of formylimidazole **1** with propargyl methanesulfonate, followed by condensation with hydroxylamine. Then CuAAC reaction between azide **14** and alkyne **16** afforded **RS161B**.

To obtain the oxime derivative **RS48B** (Scheme 7), the CuAAC reaction between alkyne derivative **15** and azido derivative **17** was performed. Amidation of ethyl glyoxylate oxime **3** with 3-azidopropyl-1-amine (20) afforded *N*-(3-azidopropyl)-2-(hydroxyimino) acetamide **17**.

Oxime Reactivation Assays— hAChE and hBChE activities were measured using a spectrophotometric assay (21) at *37 °C* (or *25 °C* for tabun conjugates) in 0.1 M sodium phosphate buffer, pH 7.4, containing 0.01% BSA and substrate acetylthio-

choline (ATCh) at 1.0 mM (hAChE) or 5.0 mM (hBChE) concentrations. OP-hAChE and OP-hBChE conjugates were prepared by incubating micromolar enzyme stocks with 4-fold molar excess of OP for 2–3 min until inhibition exceeded 95%. Inhibited enzymes and appropriate controls were passed through two consecutive size exclusion Sephadex G-50 spin columns (Roche Diagnostics) to remove excess inhibitor. The reactivation reaction was initiated by adding an oxime reactivator at 0.67 mM (or 1.0 mM for tabun conjugates) final concentrations into a nanomolar solution of OP-conjugated enzymes. Control ChE activity was measured in the presence of oxime at concentrations used for reactivation. The time course of hAChE reactivation was monitored in 96-well format by parallel consecutive assays of hAChE activity in 10 μl of reactivation mixture aliquots diluted 625 times into assay mixture containing ATCh and thiol detection reagent 5,5′-dithiobis-(2-nitrobenzoic acid). For reactivation of tabun-inhibited hAChE conventional single cuvette spectrophotometric assay was used. The first order reactivation rate constant (k_{obs}) for each oxime + OP conjugate combination was calculated by nonlinear regression
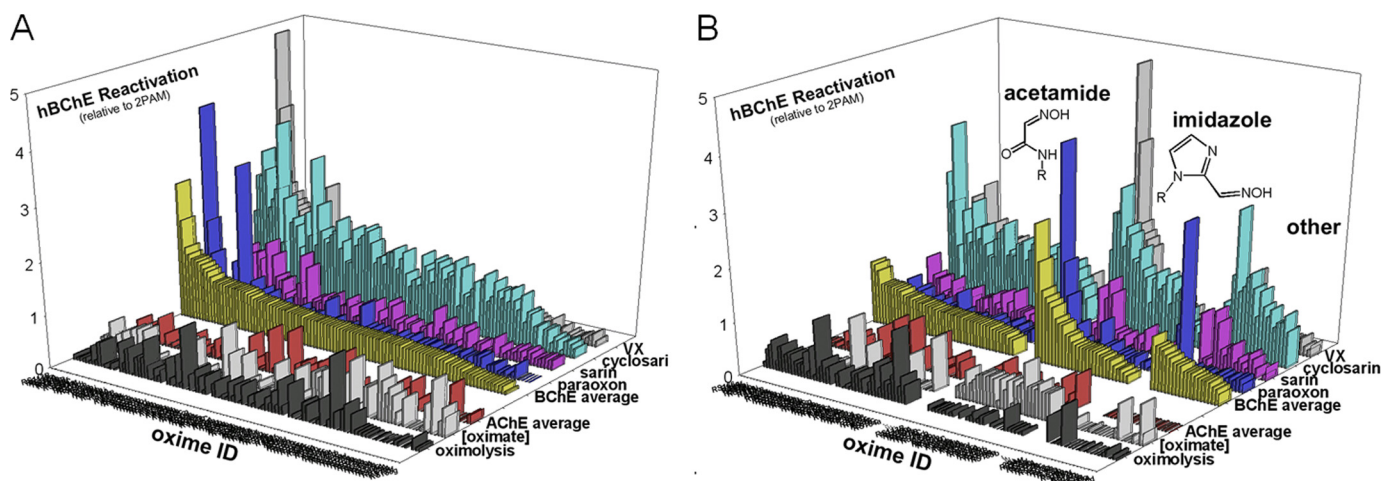
FIGURE 2. **Reactivation of VX-, cyclosarin-, sarin-, and paraoxon-inhibited hBChE by a library of 100 uncharged oxime reactivators at 0.67 mM determined by QuickScreen protocol (at 37 °C in 0.10 M phosphate buffer pH 7.4).** Reactivation potency is given relative to 2PAM. Average reactivation potency of hBChE by oximes for all four organophosphates is given as *yellow bars* and for hAChE by *red bars*. Oxime IDs are ordered by their average reactivity (*A*) and segregated by their general structure as acetamide, imidazole and other oximes (*B*). Measured nonenzymic rates of ATCh hydrolysis by oximes (3 × Δ*A*/min) and calculated fractions of oximate anion for pH 7.4 are given as *black* and *gray bars*, respectively.

as described earlier (22). Reactivation of OP-hBChE conjugates was monitored using "QuickScreen" protocol by assaying hBChE activity in the reactivation mixture in 96-well format at a single reactivation time (5 min after initiation of reactivation).

The dependence of reactivation rates on oxime concentrations and determination of maximal reactivation rate constant k_2, Michaelis-Menten type constant K_{ox}, and the overall second order reactivation rate constant k_r were conducted as previously described (22). The nonenzymic oximolysis (general base catalysis) reaction was measured for combinations of 1 mM oxime and 1 mM ATCh in buffer in the absence of enzyme. The rate was expressed from the slope of linear absorbance increase in time.

RESULTS

Reactivation of OP-hAChE Conjugates—Nearly half of the structurally diverse library of 134 uncharged oximes (supplemental Table S1) demonstrated the capacity to reactivate paraoxon-, sarin-, cyclosarin-, and VX-inhibited hAChE (Fig. 1*A*). The average reactivation efficacy for the 10 best uncharged reactivators was better than one third (34%) of 2PAM efficacy (Table 1), and three of the oximes (**RS41A**, **RS48B**, and **RS191D**) were found to be comparable with 2PAM. Reactivation trends and enhancement over 2PAM reactivation were similar for different OP conjugates (Fig. 1) with cyclosarin and VX conjugates being most amenable to reactivation, and paraoxon and tabun conjugates being noticeably more resistant to reactivation. However, the observed rank orderings were found to parallel neither computationally predicted ionization state of reactivator oxime nucleophiles nor their nucleophilic reactivity reflected in nonenzymic oximolysis of ATCh. The 56 acetamide oxime derivatives representing 41% of all tested oximes were on average equally efficient reactivators as 41 imidazole derivatives (30% of all oximes), whereas none of the varying structural scaffolds of remaining 38 oximes (29%) showed appreciable reactivation activity with average respective reactivation potencies of 0.17, 0.17, and 0.016 relative to 2PAM (Fig. 1*B*). Although within each of structural scaffolds no correlation was observed

between rates of nonenzymic oximolysis and reactivation rates, oximolysis rates of acetamide oximes were significantly larger than the ones measured for imidazole oximes or other oximes (rates as Δ*A*/min were 0.123 ± 0.011, 0.025 ± 0.002, and 0.014 ± 0.007, respectively; Fig. 1*B*). Hence, the majority of the most efficient reactivators were of the *N*-substituted 2-hydroxyimino acetamide structure (Table 1). Generally, compound structures with their oxime moiety positioned farther from the part of the molecule largely responsible for molecular recognition and binding to AChE seemed to be better reactivators. The optimal separation equivalent to a five- or six-atom linker (Fig. 1*C*) is consistent with structures of the lead **RS41A** and other top ranking reactivators (Table 1).
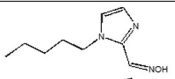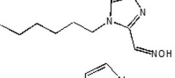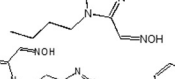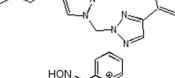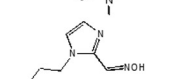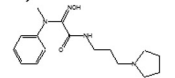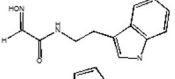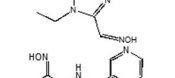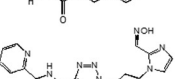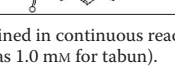
Structures of nearly half of reactivators included triazole ring (supplemental Fig. S1), but this heterocycle positioned some distance from the oxime did not significantly influence their reactivation potency. The average relative reactivation potency for 64 triazoles (*versus* 2-PAM) was 0.15 ± 0.02 (range 0.003–0.82) and for the remaining 71 reactivators 0.11 ± 0.03 (range 0–0.88), suggesting that the triazole, with its relatively strong dipole (4–5 Debye) but absent a charge at this pH, had no appreciable effect on reactivity. The triazole moiety was earlier observed to contribute synergistically to the total energy of binding of high affinity AChE inhibitors (23).

Reactivation of OP-hBChE Conjugates—Reactivation of OP-hBChE conjugates by a subset of 100 uncharged reactivators revealed a larger general enhancement of reactivation rates over those of 2PAM than observed for OP-hAChE reactivation (0.58 ± 0.04 with range 0.1–2.6 *versus* 0.14 ± 0.02 with range 0–1.3, respectively; Fig. 2). No correlation between reactivation of OP-hBChE and OP-hAChE conjugates was observed. This reflects a larger structural promiscuity of hBChE for interaction with oxime reactivators, but also a slower reactivation rate of hBChE for the reference compound, 2PAM. Accordingly, covalent OP-hBChE conjugates were reactivated, on average, similarly well by acetamide, imidazole, and other oximes (Fig. 2*B*). Seven out of ten best hBChE reactivators, however, turned to be

TABLE 2

Structures and relative potencies for OP-hBChE reactivation of 10 topmost uncharged reactivators (0.67 mM) compared with cationic pyridinium aldoxime 2PAM determined by end-point QuickScreen procedure

Nonenzymic oximolysis rates of ATCh (1 mM) by 1.0 mM oximes and calculated percentages of oximate anion and neutral species at pH 7.4 (calculated by MarvinView 5.2.6) are also given. Experiments were performed in duplicate at 37 °C in 0.10 M phosphate buffer, pH 7.4.

Oxime	Oxime structure	Reactivation* (relative to 2PAM)						Oximo lysis (dA/min)	% Oximate @ pH 7.4	% Neutral @ pH 7.4
		Avrg	POX	Sarin	CS	VX	Tabun			
RS113B		2.2	3.9	0.18	1.5	4.8	0.42	0.034	22	77
RS113A		1.6	1.7	0.28	2.3	3.4	0.40	0.019	27	73
RS115A		1.2	1.1	0.34	2.3	1.9	0.28	0.025	27	73
RS161B		1.0	0.38	0.25	2.8	1.7	0.0	0.022	56	44
2PAM		1.0	1.0	1.0	1.0	1.0	1.0	0.157	17	0.0
RS115B		0.97	0.46	1.1	1.7	1.6	0.0	0.019	34	66
RS166C		0.95	0.32	0.33	2.4	1.7	0.0	0.035	0.01	1.1
RS69F		0.92	0.38	0.91	1.8	1.5	0.0	0.121	0.11	100
RS115C		0.89	0.57	0.39	2.1	1.4	0.0	0.033	42	57
RS69A		0.84	0.31	0.20	3.3	0.37	0.0	0.152	0.38	99
RS150d		0.73	0.27	0.88	1.9	0.60	0.0	0.023	52	48

* k_{obs} values determined in continuous reactivation assay for 2PAM were: 0.052 min^{-1} (for POX), 0.13 min^{-1} (for sarin), 0.17 min^{-1} (for CS), 0.097 min^{-1} (for VX), and 0.000461 min^{-1} (as 1.0 mM for tabun).

imidazole oximes led by simple alkyl chain derivatives (Table 2). No correlation was observed between measured oximolysis rates or calculated equilibrium oximate anion concentrations with levels of hBChE reactivation.

Characterization of the Lead hAChE Reactivator RS41A—Reactivation of OP-hAChE conjugates by the overall best reactivator **RS41A** (Table 1) was additionally measured over a range of oxime concentrations, from 0.1 mM to 40 mM, and compared with uncharged (DAM and MINA) and charged (2PAM) reference compounds (Fig. 3). Although reactivation by MINA and in particular DAM was very slow, **RS41A** displayed more rapid reactivation over the entire measured concentration range, but the rate enhancement compared with the quaternary cationic 2PAM was observed largely at high oxime concentrations. This suggests that the maximal reactivation rate constant for **RS41A** is generally superior to other oximes, whereas its binding to covalent OP-hAChE conjugates (reflected in the constant K_{ox}) is not as strong as that of 2PAM (Table 3). All three uncharged oximes were characterized with large K_{ox} constants (i.e. low affinity) consistent with AChE having preference for binding cationic ligands, even in an OP-conjugated state.

The rate of **RS41A** reactivation of cyclosarin-hAChE conjugate in the pH range 6.4–8.4 did not vary significantly; however, oximolysis of ATCh by **RS41A** was 34 times faster at pH 8.4 compared with pH 6.4 (Table 4). The latter was roughly consistent with a large increase of oximate anion calculated for **RS41A** at pH 8.4 *versus* pH 6.4.

DISCUSSION

Nerve agent OPs, as well as active forms of OP-based pesticides, being small uncharged organic molecules readily diffuse through biological membranes, quickly reach the CNS and subsequently partition into brain lipids. Thus, brain AChE, although being amenable to covalent inhibition in OP poisoning, is inaccessible to the ameliorating action of commonly used pyridinium-based oxime reactivator antidotes because they are incapable of crossing the BBB due to the positive charge.

This study demonstrates that a substantial number of novel OP-hAChE reactivators emerged from a library of 134 novel, structurally diverse uncharged oximes. Promising leads with reactivation potencies comparable with the one of commonly used pyridinium reactivators, 2PAM, were singled out. Based
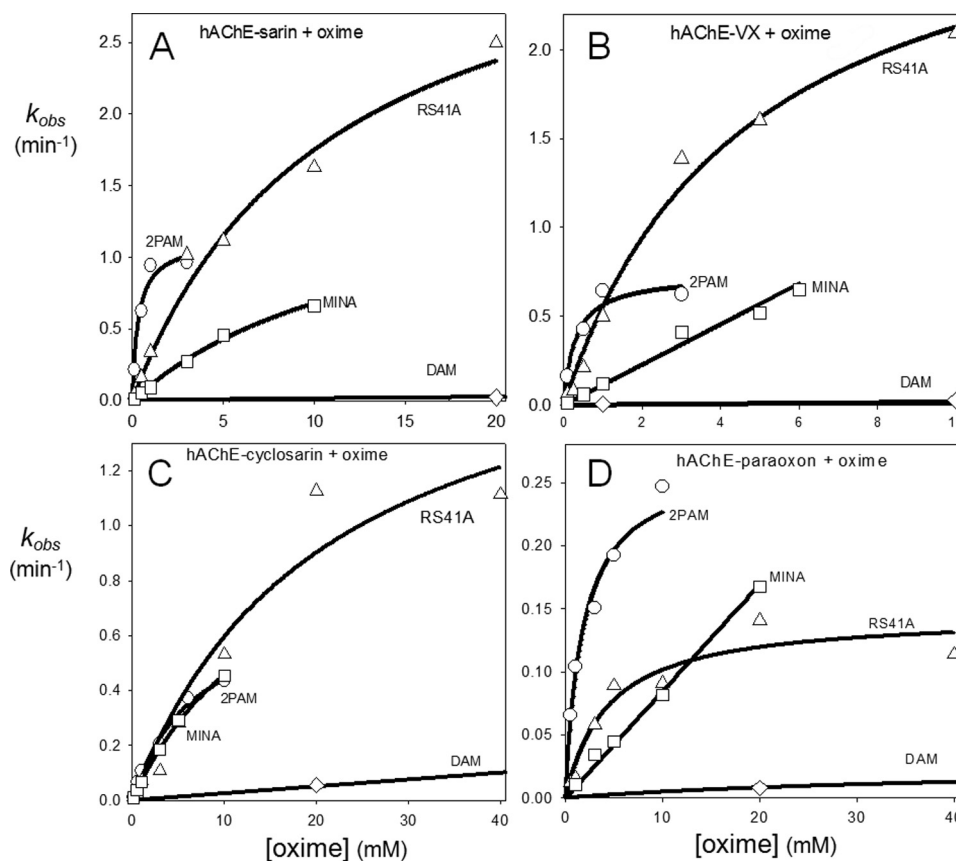
FIGURE 3. **Concentration dependence of oxime reactivation of sarin- (*A*), VX- (*B*), cyclosarin- (*C*), and paraoxon- (*D*) inhibited hAChE.** Dependence for initial lead oxime **RS41A** (△) compared with reference uncharged (DAM (◇) and MINA (□)) and cationic (2PAM (○)) oximes (measured at 37 °C in 0.10 M phosphate buffer pH 7.4) is shown.

TABLE 3

Constants for reactivation of OP-hAChE conjugates by lead reactivator RS41A and reference reactivators MINA, DAM, and 2-PAM

The maximal reactivation rate constant (k_2), the Michaelis-type dissociation constant of OP-hAChE-oxime complex (K_{ox}), and overall second order reactivation rate constant (k_r) were calculated by nonlinear regression from plots presented in Fig. 3. Experiments were done in duplicate or triplicate at 37 °C in 0.10 M phosphate buffer, pH 7.4, and are summarized as shown in Fig. 3.

OP	Sarin			VX			Cyclosarin			Paraoxon		
oxime	k_2 (min⁻¹)	K_{ox} (mM)	k_r (M⁻¹ min⁻¹)	k_2 (min⁻¹)	K_{ox} (mM)	k_r (M⁻¹ min⁻¹)	k_2 (min⁻¹)	K_{ox} (mM)	k_r (M⁻¹ min⁻¹)	k_2 (min⁻¹)	K_{ox} (mM)	k_r (M⁻¹ min⁻¹)
RS 41A	3.7 ± 0.7	11 ± 4	340 ± 61	3.1 ± 0.3	4.6 ± 0.9	670 ± 77	1.9 ± 0.3	21 ± 8	88 ± 18	0.15 ± 0.02	4.3 ± 1.7	34 ± 11
MINA	1.6 ± 0.4	14 ± 5	120 ± 14	> 1.0	> 10	110 ± 8	1.2 ± 0.6	16 ± 12	75 ± 17	> 0.20	> 20	8.4 ± 0.3
DAM	0.13 ± 0.03	88 ± 29	1.5 ± 0.2	> 0.1	> 20	1.7 ± 0.1	> 0.1	> 40	2.5 ± 0.2	0.027 ± 0.015	46 ± 59	0.59 ± 0.47
2PAM	1.1 ± 0.1	0.34 ± 0.16	3300 ± 1300	0.73 ± 0.09	0.30 ± 0.14	2300 ± 800	0.73 ± 0.10	6.6 ± 1.7	110 ± 16	0.27 ± 0.03	1.8 ± 0.6	150 ± 35

TABLE 4

pH dependence of reactivation of VX-inhibited hAChE by lead oxime RS41A (1.0 mM), oximolysis of 1 mM ATCh by RS41A, and calculated concentration of oximate anion for RS41A (calculated by MarvinView 5.2.6)

Triplicate experiments (given is mean ± S.D.) were done in 0.1 M phosphate buffers.

	Reactivation		Oximolysis		[Oximate] @pH	
pH	k_{obs}	Ratio	Rate	Ratio		Ratio
	min⁻¹		*ΔA/min*		*%*	
6.4	0.19 ± 0.01	1	0.023 ± 0.003	1	0.02	1
7.4	0.16 ± 0.03	0.84	0.120 ± 0.007	6	0.20	10
8.4	0.17 ± 0.05	0.89	0.760 ± 0.096	34	1.5	75

on the *in vitro* data, the lead reactivator, oxime **RS41A**, is expected to reactivate OP-hAChE conjugates *in vivo* in blood and simultaneously enter the CNS and reactivate inhibited brain hAChE. The concentration dependence of **RS41A** reactivation with its respectable maximal reactivation rates (large

k_2; Table 3) but relatively weak binding to OP-hAChE conjugates (large K_{ox}, Table 3) indicates that the lead molecule is amenable to further structural refinement to gain higher reactivation potency. Modifying the size and character of both the aliphatic linker and the heterocycle of **RS41A** clearly affects

reactivation (Table 1). Several discrete structural variations leading to compounds **RS191D**, **RS191C**, and **RS186B** exhibited minimal or slight reductions in overall reactivation potency compared with **RS41A**. However, this should enable us systematically to vary the structure of the heterocyclic ring and its distance from the oxime and then examine the influence of the α-keto and α-carbamoxy moieties.

Structural diversity of OP-hAChE conjugates on the other hand was reflected in reactivation trends, as well. Although varying oxime structures seemed to affect reactivation of methylphosphonyl OP-hAChE conjugates (derived from sarin, cyclosarin, and VX inhibition) in a similar way, tabun- and paraoxon-derived conjugates with larger phosphorus substituents occupying the OP-hAChE acyl pocket had different structural requirements and proved more refractory to reactivation. This indicates that the most effective of our reactivators preferably approach the conjugated phosphorus directly from the active center gorge opening and the acyl pocket and not from the direction of the hAChE choline binding site. In support of this conclusion, reactivation of OP-hBChE conjugates sharing a larger acyl pocket space and active center gorge opening did not indicate faster reactivation of methylphosphonates.

The lack of noticeable influence of intrinsic nucleophilic oxime reactivity (reflected in nonenzymic ATCh oximolysis experiments) as well as ionization state of the oxime moiety (reflected in pH dependence experiments) on the overall oxime-assisted reactivation emphasizes a decisive influence of proper binding complementarity of reactivator molecules with the environment of the active center gorge opening of OP-hAChE conjugates.

Scheme A shows ionization equilibria of amino oximes centered around physiological pH values and the corresponding ionization species. Depending on the pK_a values for the amine and the oxime functionalities, both a zwitterionic and neutral species could form with an increase in pH. Although the oximate formed by ionization equilibration of **RS41A** (Scheme A) may be the better nucleophile, the active center may be limiting access to a zwitterionic or anionic species. By examining reactivity for a series of *N*-substituted 2-hydroxyimine acetamides as a function of pH, it may be possible to select an agent that increases the fraction of the reactive species to cross the BBB, yet allows a sufficient fraction of reactivator with a higher binding affinity to interact in the active center gorge. Our future refinement strategies for improvement of **RS41A** reactivity will therefore be based on achieving higher degree of steric and electrostatic complementarity between three-dimensional structures of hAChE conjugates and reactivator molecules. Our reactivation data for OP-hBChE conjugates further support this approach. Oxime structure requirements for the efficient reactivation of hBChE, although structurally and functionally a very close relative of hAChE, are clearly very different (Figs. 1 and 2 and Tables 1 and 2), showing that relatively moderate variations of the active center gorge size and shape in two enzymes have substantial consequences for forming productive complementary fits of small reactivator molecules into OP-conjugated enzymes.

The value of timely recovery of inhibited brain AChE was clearly demonstrated recently through increased survival and reduction of seizures and status epilepticus in OP-exposed guinea pigs (11) upon administration of pro-2PAM, an uncharged centrally active analog of commonly used reactivator 2PAM. Enzymatic conversion of pro-2PAM into 2PAM, upon its diffusion into CNS is key to functionality of the pro-drug concept whose maximal reactivation efficacy is limited to the efficacy of 2PAM. Initial reports of an alternative approach of conjugating pyridinium aldoximes to glucose where reactivator molecules rely on active transport of glucose into CNS, instead of simple diffusion, have also proved promising for *in vitro* reactivation experiments (9, 10) where 2PAM reactivation levels were approached but not exceeded. These oxime derivatives displayed very low *in vivo* toxicities. Finally, cationic oximes encapsulated into nanoparticle drug delivery system capable of penetrating the BBB (24, 25) need to be optimized for fast release of therapeutically efficient doses into CNS to prove their efficiency. The maximal efficacy for all of these approaches depends on the intrinsic efficacy of involved respective pyridinium aldoximes.

In contrast, our approach is based on designing small organic nucleophilic molecules unrelated to pyridinium aldoximes and devoid of permanent positive charge, but amenable to protonation. The uncharged form of reactivators should spontaneously diffuse into CNS. While in ionization equilibrium, the protonated amine form is efficiently attracted to the electron-rich active center environment of the inhibited AChE. We are thus able to gauge independently two distinct molecular properties essential for the overall efficacy, CNS penetration and intrinsic reactivation potency.

REFERENCES

1. Sekijima, Y., Morita, H., Shindo, M., Okudera, H., and Shibata, T. (1995) *Rinsho Shinkeigaku* **35,** 1241–1245 (in Japanese)
2. Yanagisawa, N., Morita, H., and Nakajima, T. (2006) *J. Neurol. Sci.* **249,** 76–85
3. Nozaki, H., Hori, S., Shinozawa, Y., Fujishima, S., Takuma, K., Sagoh, M., Kimura, H., Ohki, T., Suzuki, M., and Aikawa, N. (1995) *Inten. Care Med.* **21,** 1032–1035
4. Okumura, T., Takasu, N., Ishimatsu, S., Miyanoki, S., Mitsuhashi, A., Kumada, K., Tanaka, K., and Hinohara, S. (1996) *Ann. Emerg. Med.* **2,** 129–135
5. Taylor P. (2011) in *Goodman & Gilman's The Pharmacological Basis of Therapeutics* (Brunton, L. L., Chabner, B., and Knollman, B., eds) 13th Ed., pp. 239–254, McGraw-Hill, New York
6. Skovira, J. W., O'Donnell, J. C., Koplovitz, I., Kan, R. K., McDonough, J. H., and Shih, T. M. (2010) *Chem. Biol. Interact.* **187,** 318–324
7. Shih, T. M., Skovira, J. W., O'Donnell, J. C., and McDonough, J. H. (2010) *J. Mol. Neurosci.* **40,** 63–69
8. Shih, T. M., Duniho, S. M., and McDonough, J. H. (2003) *Toxicol. Appl. Pharmacol.* **188,** 69–80
9. Heldman, E., Ashani, Y., Raveh, L., and Rachaman, E. S. (1986) *Carbohydr. Res.* **151,** 337–347
10. Garcia, G. E., Campbell, A. J., Olson, J., Moorad-Doctor, D., and Morthole, V. I. (2010) *Chem. Biol. Interact.* **187,** 199–206
11. Demar, J. C., Clarkson, E. D., Ratcliffe, R. H., Campbell, A. J., Thangavelu, S. G., Herdman, C. A., Leader, H., Schulz, S. M., Marek, E., Medynets, M. A., Ku, T. C., Evans, S. A., Khan, F. A., Owens, R. R., Nambiar, M. P., and Gordon, R. K. (2010) *Chem. Biol. Interact.* **187,** 191–198
12. Bodor, N., Shek, E., and Higuchi, T. (1975) *Science* **190,** 155–156
13. Amitai, G., Adani, R., Yacov, G., Yishay, S., Teitlboim, S., Tveria, L., Limanovich, O., Kushnir, M., and Meshulam, H. (2007) *Toxicology* **233,** 187–198
14. Cossrow, J., Guan, B., Ishchenko, A., Jones, J. H., Kumaravel, G., Lugovs-

koy, A., Peng, H., Powell, N., Raimundo, B. C., Tanaka, H., Vessels, J., Wynn, T., and Xin, Z. (June 30, 2008) U. S. Patent 20,090,005,359:01

15. Nicolaides, D. N., Litinas, K. E., Papamehael, T., Grzeskowiak, H., Gautam, D. R., and Fylaktakidou, K. C. (2005) *Synthesis* **3,** 407–410

16. Rostovtsev, V. V., Green, L. G., Fokin, V. V., and Sharpless, K. B. (2002) *Angew. Chem. Int. Ed.* **41,** 2596–2599

17. Beccalli, E. M., Borsini, E., Broggini, G., Palmisano, G., and Sottocornola, S. (2008) *J. Org. Chem.* **73,** 4746–4749

18. Stefely, J. A., Palchaudhuri, R., Miller, P. A., Peterson, R. J., Moraski, G. C., Hergenrother, P. J., and Miller, M. J. (2010) *J. Med. Chem.* **53,** 3389–3395

19. Kalisiak, J., Sharpless, K. B., and Fokin, V. V. (2008) *Org. Lett.* **10,** 3171–3174

20. Asati, A., Santra, S., Kaittanis, C., Nath, S., and Perez, J. M. (2009) *Angew. Chem. Int. Ed.* **48,** 2308–2312

21. Ellman, G. L., Courtney, K. D., Andres, V., Jr., and Featherstone, R. M. (1961) *Biochem. Pharmacol.* **7,** 88–95

22. Kovarik, Z., Radić, Z., Berman, H. A., Simeon-Rudolf, V., Reiner, E., and Taylor, P. (2004) *Biochemistry* **43,** 3222–3229

23. Manetsch, R., Krasiñski, A., Radić, Z., Raushel, J., Taylor, P., Sharpless, K. B., and Kolb, H. C. (2004) *J. Am. Chem. Soc.* **126,** 12809–12818

24. Kufleitner, J., Worek, F., and Kreuter, J. (2010) *J. Microencapsul.* **27,** 594–601

25. Wagner, S., Kufleitner, J., Zensi, A., Dadparvar, M., Wien, S., Bungert, J., Vogel, T., Worek, F., Kreuter, J., and von Briesen, H. (2010) *PLoS One* **5,** e14213